ACS APPLIED NANO MATERIALS

www.acsanm.org

Forum Article

A Roadmap for Mechanically Interlocked Molecular Junctions at Nanoscale

Chaoqing Yang and Hongliang Chen*

Cite This: *ACS Appl. Nano Mater.* 2022, 5, 13874−13886

Read Online

ACCESS | Metrics & More | Article Recommendations

ABSTRACT: The beauty and utility of mechanically interlocked architectures have received considerable notice from scientists in the past several decades. Plentiful scientific and technological achievements have been made and developed because of conjoining mechanically interlocked molecules (MIMs) and molecular electronic devices at nanoscale. The interaction mechanisms and translational dynamics of various MIMs, e.g., rotaxanes, catenanes, and daisy chains, have been investigated systemically through different experimental methods. On account of the recent advances of single-molecule techniques, the electrical and mechanical performance of mechanically interlocked molecular junctions (MIMJs) or nanodevices have been explored in a timely manner. In this Review, we survey the field of MIMs from a perspective of unique structural properties including topological features, translational dynamics, bistable switching properties, insulation effects, and dynamic stability present in MIMs. We then give a fundamental description of electron transport mechanisms in MIMJs for three different nanodevice geometries: (i) monolayer switching tunnel junctions (MSTJs), (ii) single-molecule junctions (SMJs) based on MIMs, and (iii) real-time transistor-like platforms.

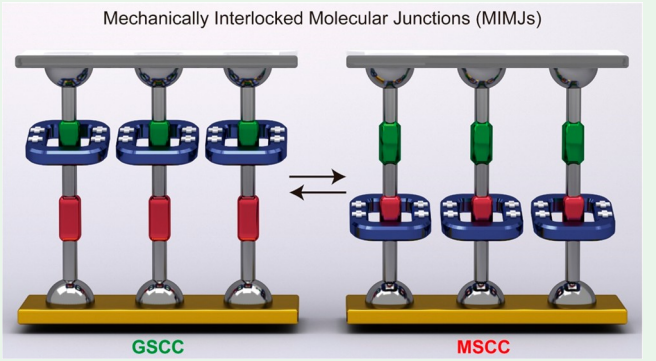

KEYWORDS: *mechanically interlocked molecules (MIMs), rotaxanes, catenanes, molecular electronics, single-molecule devices, nanodevices*

1. INTRODUCTION

Three scientists, Jean-Pierre Sauvage,[1] J. Fraser Stoddart,[2] and Bernard L. Feringa,[3] were awarded the 2016 Nobel Prize in Chemistry jointly for their pioneering work in the design, synthesis, and investigation of molecular machines (Figure 1), i.e., molecular switches,[4] molecular pumps,[5] molecular rotors,[6] and nanocars.[7] Mechanically interlocked molecules (MIMs) represent a huge family of molecular machines that are constructed with mechanical bonds.[8] The interlocked structures and translational dynamics of MIMs endow them with fascinating switching properties. For example, for a [2]catenane-type molecular machine, the bistable switching properties can be controlled finely by external chemical or electrical stimuli.[9] The co-conformational change of a [2]rotaxane can be tuned in a controlled manner by chemical or electrochemical methods.[10] The [2]daisy chain also presents bistable features between stretched and contracted states with a stimulus from metal ions.[11] After the synthesis and construction of different kinds of MIMs in past decades, MIMs are beginning to evolve from objects of basic synthetic chemistry and plain topological structure toward functional systems or devices.[12]

Co-conformational changes will therefore lead to changes in electronic structures and result in either a high- or low-conductance state when they are connected in electronic devices. This phenomenon represents the foundation of molecular machines for their application in molecular electronics, leading to the rise of single-supramolecular electronics (SSEs).[13] The focus on SSEs is to investigate the noncovalent interactions, i.e., $\pi-\pi$ interactions,[14] hydrogen bonding,[15] and host−guest interactions,[16] in supermolecules and MIMs and their influence on the charge transport characteristics.[12,17−20] The development of single-molecule techniques in the past decade, such as single-molecule force spectroscopy[21−25] and graphene single-molecule junctions,[26−29] has promoted the prosperity of SSEs. For example, single-molecule junctions based on rotaxanes have been used to gain a deep understanding of the effect of torsion angles on electrical conduction in MIMs.[30] Bistable [2]catenanes and [2]rotaxanes have been used to construct solid-state electronically monolayer switching tunnel junctions (MSTJs) in

Special Issue: Professor Sir Fraser Stoddart's 80th Birthday Forum

Received: April 29, 2022
Accepted: June 20, 2022
Published: July 5, 2022

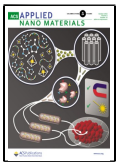

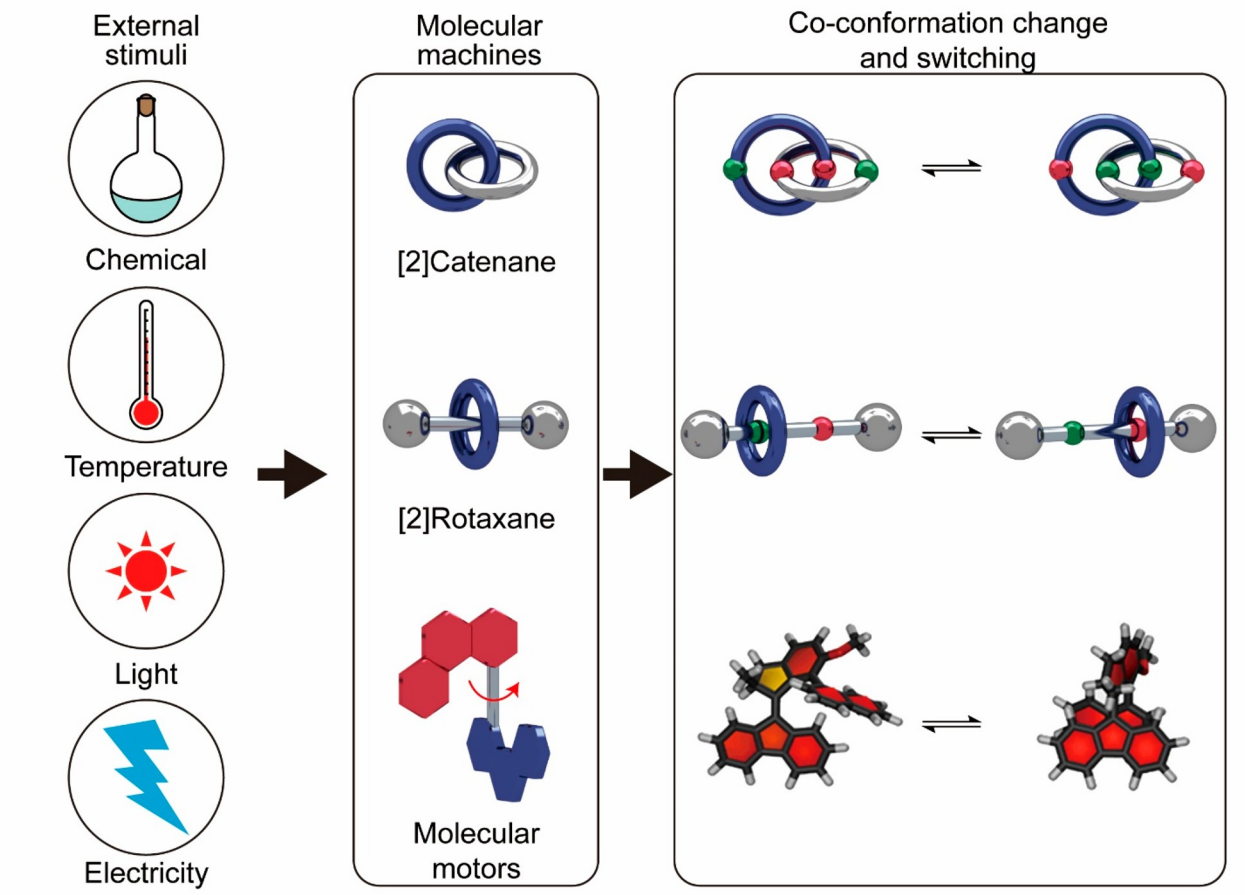

Figure 1. Schematic representations of the variable conformational changes of three kinds of molecular machines: [2]catenane, [2]rotaxane, and a molecular motor under external stimuli.

crossbar devices.[31] These MSTJ devices show remnant molecular electronic signatures and nonvolatile memory effects in high-density integrated circuits.[31−38]

Numerous excellent reviews have been published covering different kinds of MIMs, i.e., bistable rotaxanes,[39] switchable catenanes,[40] interlocked daisy chains,[41] and artificial molecular machines.[42] In this Review, we summarize briefly the properties of MIMs and then focus on recent developments in mechanically interlocked molecular junctions (MIMJs). We first summarize the structural characteristics of MIMs, i.e., the topological features, different co-conformations, translational motion dynamics, bistable switching properties, insulating effects, and dynamic stability. We then provide a historical overview of MSTJs developed by Stoddart and co-workers. We also discuss electron transport properties in MIMs related to multiple noncovalent interactions in MIMs. Finally, we tentatively discuss the potential technical challenges and possible technology roadmap.

2. STRUCTURAL FEATURES OF MIMS

Mechanically interlocked architectures contain a number of discrete molecular subunits or components. The most fascinating feature of MIMs is the mechanical bond which denotes an entangled state between different components. These components of MIMs hold together unless the chemical bonds between the different components are broken.[2] It is the physical behavior that endows MIMs with various features that can be employed to make single-molecule electronic devices.

2.1. Topological Features of MIMs. Several basic components such as rings and wires and large terminal groups are used to construct MIMs (Figure 2).[43] Molecular wires and

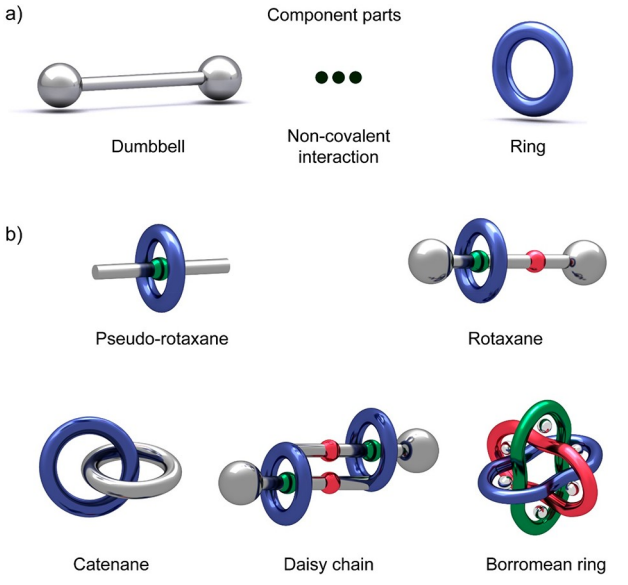

Figure 2. (a) Schematic illustration showing the component parts of MIMs. (b) Cartoon models of MIMs with different topologies. Reprinted with permission from ref 13. Copyright 2021, Springer Nature Limited.

https://doi.org/10.1021/acsanm.2c01880
ACS Appl. Nano Mater. 2022, 5, 13874−13886

molecular rings are not only ubiquitous, they are also abundant. Different combinations of the component parts open up architectures involving many different nanotopologies.[44] The dumbbell-shaped configuration of a rotaxane involves one or more rings that are threaded through a wire, and two larger stoppers prevent the rings from exiting the wire. If a linear axle traverses a macrocycle without bulky stoppers at the ends, the supramolecular complex is referred to as a pseudorotaxane.[45] The basic configuration of a catenane is a molecule with two interlocked rings. If the ring of a [2]rotaxane connects covalently with its dumbbell, a different architecture, a molecular daisy chain, occurs.[46] More graceful advanced structures, i.e., a trefoil knots,[47] Borromean rings,[48] olympiadane,[49] and molecular handcuffs,[43] have been made in the past several decades and applied in various functional materials.[50,51]

2.2. Translational Motion and Circumrotation of MIMs. Considering the additional degrees of freedom originating from choreographed mechanically interlocked architectures, MIMs are perfect exhibitions of molecular motions triggered by external stimuli, such as chemicals,[52] electricity,[53−55] and light[56,57] (Figure 3). When a macrocyclic

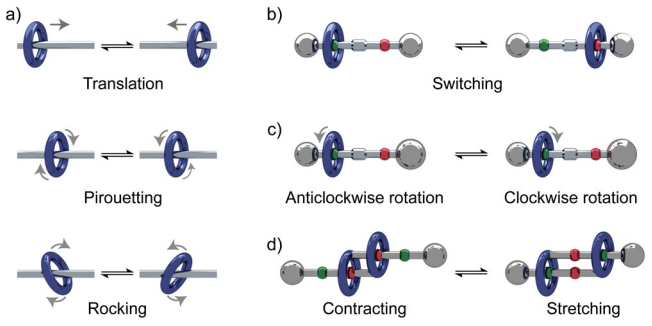

Figure 3. (a) Schematic illustration showing three kinds of dynamic motions: translation (top), pirouetting (middle), and rocking (bottom) in interlocked molecular structures. The (b) switching property and (c) mechanically planar chirality of a [2]rotaxane. (d) The mechanical contraction and stretching of a [2]daisy chain.

molecule encircles a molecular axle, either a molecular ring in catenane or a molecular dumbbell in rotaxane, three kinds of intramolecular motions occur. The first process is an intramolecular translational motion: a molecular ring moves along the molecular axle (Figure 3a, top). The second situation is an intramolecular pirouetting motion; that is to say, the molecular ring rotates regularly along the molecular axle (Figure 3a, middle). The last process is intramolecular rocking motion: the molecular ring and molecular wire swivel orthogonally because of their steric interactions (Figure 3a, bottom). In the case of a [2]rotaxane, the molecular ring travels regularly back and forward between two recognition sites at a fast pace[58] (Figure 3b), or the molecular ring rotates freely with respect to the molecular dumbbell[59] (Figure 3c). In a [2]rotaxane with planar chirality, however, the rotation of the molecular ring involves two kinds of situations, along the clockwise or the anticlockwise directionality (Figure 3c). In the case of a [2]catenane, a molecular ring can rotate relative to another ring, or two molecular rings move closer to each other.[60] In the case of a [2]daisy chain, the molecular wires are cross-threaded into the molecular rings (Figure 3d), and the interlocked [2]daisy chain exhibits alternant stretched or contracted states in defined dimensions, which is considered to be artificial molecular muscles.[11] These reversible dynamic motions of MIMs can be utilized to make electronic devices.

2.3. Bistable Switching of MIMs. The bistability of MIMs is the basis for the construction of single-molecule devices. When a MIM exists as two states at equilibrium, namely, the ground-state co-conformation (GSCC) and the metastable state co-conformation (MSCC), the MIM may show a bistable switching and memory effect.[61] Different from the switching mechanism existing in other monolayer junctions based on ferroelectric polymers[62] or molecular rotors,[63] the design of switching MIMs depends on the incorporation of many different recognition sites (Figure 4a). As illustrated in Figure 4, degenerate (Figure 4b, left) and nondegenerate (Figure 4c, left) MIMs are used to explain the phenomenon of translational isomerism. In a degenerate donor−acceptor [2]rotaxane, the molecular ring travels regularly and quickly back and forward between two identical recognition sites.[2] In a nondegenerate [2]rotaxane, however, one of the recognition units is more attractive to the molecular ring than the other.[8]

The underlying law associated with the kinetic and thermodynamic control of the co-conformational change is provided by plotting the free energy ($\Delta G^{\ddagger}$) profiles (Figure 4b,c). No difference in free energies is observed in the energy profile of degenerate [2]rotaxane when the molecular ring encloses either of the two identical recognition sites (Figure 4b, right). For nondegenerate [2]rotaxane, however, there is an obvious additional energy term (ΔG^{0}), which originates from the different free energy of two molecular conformations (Figure 4c, right). One is the globally most stable mechanostereoisomer, which is called the GSCC. The other is the locally stable mechanostereoisomer, which is known as the MSCC. The ratio of molecules in the GSCC to those in the MSCC is used to describe the dimensionless co-conformational equilibrium constant (K_{eq}). Normally, the value is more than 1, which means that this kind of MIM prefers the GSCC state. Digital simulation based on the computational chemistry giving more and foreseeable information is often used as a complementary tool to investigate the kinetic and thermodynamic parameters of bistable molecular switches.[64]

Component parts of MIMs have been optimized continuously to achieve precise control over bistable switching (Figure 4d,e). One method is to adjust the distance between two different recognition units by using a molecular spacer, such as a glycol or terphenylene unit (Figure 4d).[65] However, it is difficult to explain clearly the influence of molecular spacers on the kinetics of bistable MIMs, because the enthalpic and entropic parameters in different molecular co-conformations are not so easily obtained.[12] Another strategy is to insert a functional unit of speed bumps between two molecular recognition sites, so the lifetimes of the MSCC and GSCC states are artificially adjusted (Figure 4e).[66] The incorporation of an electrostatic barrier, for example, a dicationic bipyridinium ($BIPY^{2+}$) subunit, as a speed bump in a [2]rotaxane can change the free energy ($\Delta G^{\ddagger}$) and increase the lifetime from the MSSC to the GSCC state.[67] In another case, light-responsive azobenzene units are used as a steric barrier to construct a light-switchable bistable [2]rotaxane.[68]

2.4. Insulating Effects of MIMs. Threading a linear molecular conductor inside an insulating molecular sheath provides an efficient method to construct insulated molecular wires.[69] One strategy for achieving insulating effects of MIMs is to construct a pseudopolyrotaxane or polyrotaxane (Figure

https://doi.org/10.1021/acsanm.2c01880
ACS Appl. Nano Mater. 2022, 5, 13874−13886

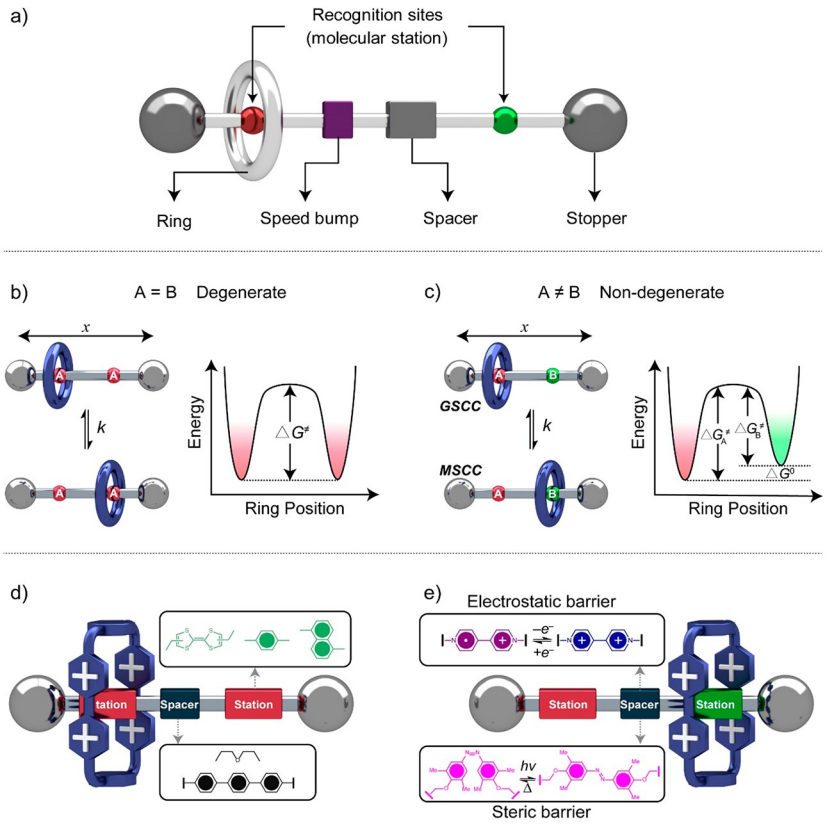

Figure 4. (a) Schematic illustration showing the component parts of a switchable [2]rotaxane. (b, c) Schematic illustration showing the co-conformational changes and energy diagrams of (b) degenerate and (c) nondegenerate [2]rotaxane. GSCC: ground-state co-conformation; MSCC: metastable state co-conformation; $\Delta G^{\ddagger}$: free energy. (d) Schematic illustration showing an additional molecular spacer unit positioned between two recognition sites of a [2]rotaxane. (e) Introduction of two kinds of speed bumps between two recognition sites of MIMs.

5a).[70] The insulated structures of MIMs have several advantages on improving the properties of MIMs.[71] First, insulated MIMs can increase the luminescence stability of the centered axils. Anderson and co-workers made an insulated [2]rotaxane in which a cyanine dye is encapsulated by a α-cyclodextrin (Figure 5b).[72] The stability toward photo-oxidation of the insulated [2]rotaxane is 40-fold higher than that of the free cyanine molecules, which might originate from the fact that cyclodextrin encapsulation protects the centered axil in its excited state.[72] Second, insulated MIMs can adjust electron transport behavior between a linear molecular conductor and its external redox centers (Figure 5c).[73] The Stern–Volmer quenching constant of this [3]rotaxane is slower than that of the free π-system because of the electrostatic shielding effect by the cationic molecular shells and the steric shielding effect.[73] Third, the insulated structures of MIMs show high fluorescence efficiency (Figure 5d). The fluorescence efficiencies of solid poly(*p*-phenylene),[74] poly-(4,4′-diphenylenevinylene),[75] and polyfluorene encapsulated by α- or β-cyclodextrin rings are generally two or three times higher than the value of free dumbbells. This phenomena can be attributed to the buffer zone provided by the insulated MIMs to avoid the exciton coupling.[76] Last but not least, the special design of [2]rotaxane with sterically shielding groups is used to improve the stability of a conjugated oligoyne chain during the conductivity measurement.[77] Nichols and co-workers prepared a [2]rotaxane which is constructed with an oligoyne dumbbell with two bulky 3,5-diphenylpyridine stoppers and a macrocycle containing phenanthroline. The results of conductivity measurements at room temperature show that the threaded macrocycle along the dumbbell wire has only a minimal impact on the conductance. The junction formation probability of the dumbbell in the absence of the macrocycle, however, is obviously lower than the [2]rotaxane junction.

2.5. Dynamic Stability of MIMs. Over the past several decades, many kinds of molecules have been linked to different electrodes, such as gold,[17,19,20] graphene,[78] carbon nanotubes,[79] and liquid-metal.[80] In conventional rigid molecular wires (Figure 6a) based on break-junction techniques, molecules are attached to Au electrodes through covalent,[81] dative,[82] or electrostatic[83] anchors. Upon slight mechanical perturbation, however, the molecular junction breaks because of the lack of moving freedom of the rigid molecular backbone.[84] To solve this problem, $\pi-\pi$ dimers are employed to construct soft supramolecular junctions (Figure 6b).[85,86] In these junctions, either of the two molecules connects to the electrode at one end,[87] and the bonding strength between the molecule and electrode is stronger than that of $\pi-\pi$ dimers.[14] The π-stacked kernel has shown relatively high slipping freedom by slowly separating the two electrodes, leading to destructive quantum interference and large on/off ratios.[88,89] Supramolecular junctions based on $\pi-\pi$ dimers, however, suffer from weak noncovalent bonding strength. It is still a challenge to control the aggregation of molecules. Furthermore, the $\pi-\pi$ stacking is fragile to the change of external environment.[90]

https://doi.org/10.1021/acsanm.2c01880
ACS Appl. Nano Mater. 2022, 5, 13874−13886

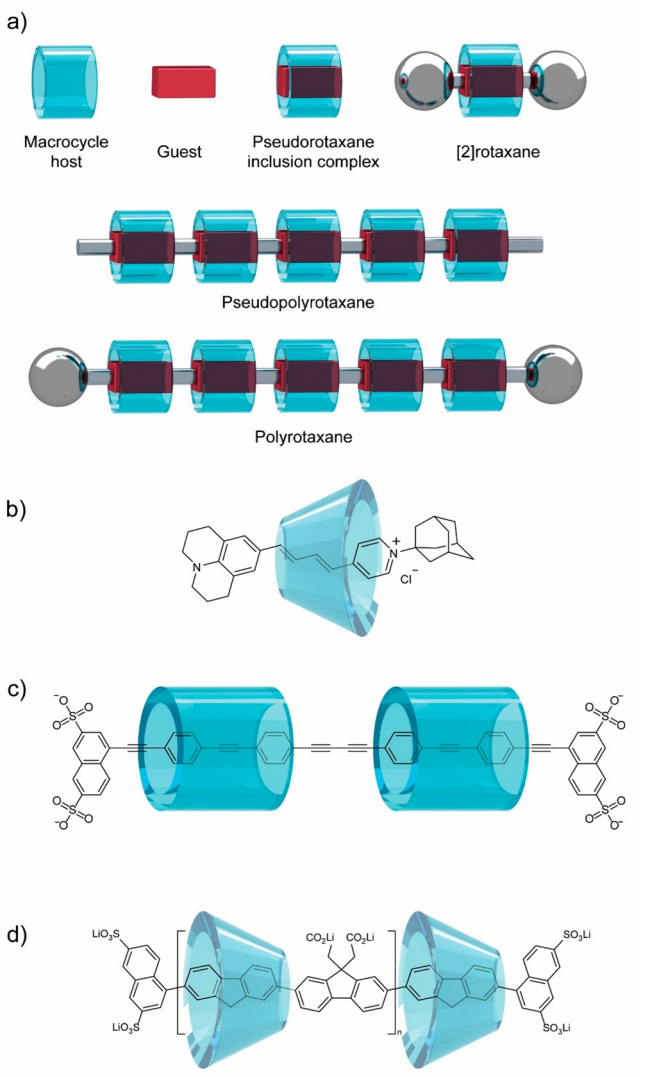

Figure 5. (a) The construction of insulated molecular wires based on MIMs. (b) Molecular structure of a [2]rotaxane consisting of cyanine dye threaded through α-cyclodextrin. (c) Schematic diagram showing [3]rotaxane consisting of an anionic phenylene ethynylene dumbbell threaded through two cationic cyclophanes. (d) Schematic diagram showing polyrotaxanes based on polyfluorene. Reprinted with permission from ref 69. Copyright 2007, Wiley.

Different topologies, versatile co-conformations, and multiple functionalities of MIMs offer MIMJs more advantages over conventional molecular junctions (Figure 6c). The intrinsic motion features of MIMs endow them abundant dynamics during the process of formation and evolution of MIMJs. For example, in a molecular junction based on a [2]catenane,[24] the interlocked structure ensures the stability of the architecture. The mechanical bond, however, provides the moving dynamics between the two rings. The dynamic stability provides a soft stable contact between the MIMs and electrodes, shedding light on the fabrication of stable molecular devices.

3. MONOLAYER SWITCHING TUNNEL JUNCTIONS (MSTJS) BASED ON MIMS

Monolayer switching tunnel junctions (MSTJs) based on MIMs have been developed by Stoddart, Heath, and coworkers since the 1990s (Figure 7a–c).[31,37] MSTJs adopt a vertical two-terminal three-layer device geometry in which a single layer of MIMs is inserted between a top and a bottom electrode. Polysilicon (Si) is chosen as the bottom electrode for three reasons.[91−93] First, elemental silicon in the Periodic Table is directly below carbon, which allows ohmic contact with organic molecules. Second, the stability of the Si electrodes reduces the formation of conducting filaments even at high voltages. Third, Si materials, which are widely used in integrated circuits, are compatible with current semiconductor manufacturing technology.

The monolayer of bistable MIMs, obtained by the Langmuir−Blodgett (LB) technique, is introduced on top of the Si bottom electrodes. Titanium (Ti) top electrodes are deposited at right angles by sputtering hot Ti metal atop the monolayer of MIMs with the aid of a mask (Figure 7b,c).[31,36] The LB method has tremendous flexibility, which can control the coverage and density of molecules and allow the tight packing.[94] The hydrocarbon chains in the bistable [2]-catenanes or the hydrophobic terminals in the bistable [2]rotaxanes together protect the monolayer of MIMs from being damaged during the deposition on top of the electrodes. This protecting mechanism can be confirmed by the bonding between the Ti electrodes and hydrocarbon chains in MIMs using reflection absorption infrared spectroscopy.[37]

The switching of MSTJs is an electrochemically driven transformation between the GSCC and the MSCC state (Figure 7d). The transformation from GSCC to MSCC corresponds to the oxidation of neutral tetrathiafulvalene (TTF) to TTF dication (TTF^{2+}), which has been demonstrated to proceed relatively fast.[12] If the external stimulus reduces the TTF^{2+} dication back to its neutral form, the transformation from MSCC to GSCC state happens. The relaxation time from MSCC to GSCC is an important parameter, because it determines the retention time of a memory bit (or the volatility of a switch) of the two-terminal MSTJs.[95] When the write voltage pulses of crossbar MSTJ devices reach a level of +2 V, the molecular switch is in a closed state. In this case, most of the molecules are in MSCC state with low resistance. As illustrated in Figure 7e, the binary information can be stored in the tested portion, which corresponds to ASCII characters for "CIT" (Figure 7e).[31]

The choice of electrode materials in an MSTJ device is important for the tested molecular information. The Hewlett-Packard research group (HP) also fabricates and tests a set of MSTJ devices by using a similar route, the similar amphiphilic MIMs, and the same LB technique.[96] There is a difference between the HP and Caltech devices; that is, the HP group used platinum (Pt) as the bottom electrode.[97] Although large amplitudes of switching (high bias) are observed in HP devices, the switching behavior is independent of temperature, revealing that HP devices are a kind of physical mechanism instead of the chemical nature of the MIMs that dominate the electron transport.[98]

These observations demonstrate that the choice of electrode materials and manufacturing methods are vital to the stability, functionality, and robustness of MSTJs. Some recent advances in nanofabrication methods have shed light on the renaissance of MSTJs. First, Stoddart, Guo, and colleagues demonstrated a planar device geometry in which a single-layer graphene nanosheet is employed as the conducting channel (Figure 7f).[99] Single-layer bistable [2]rotaxanes are self-assembled on top of the graphene layer through noncovalent $\pi-\pi$ interaction between the pyrene unit and the graphene. The special

https://doi.org/10.1021/acsanm.2c01880
ACS Appl. Nano Mater. 2022, 5, 13874−13886

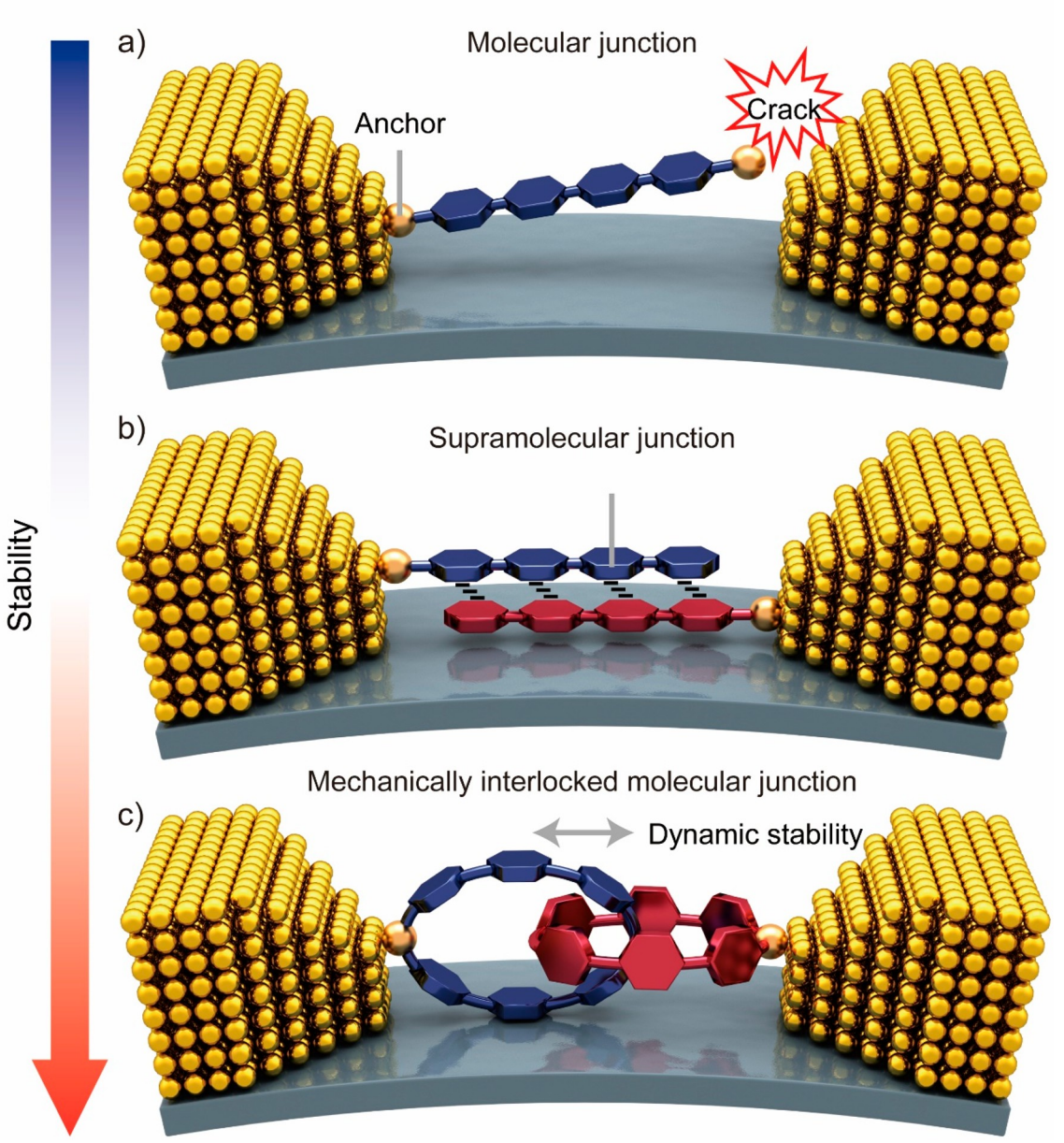

Figure 6. Schematic illustration showing (a) a rigid molecular junction, (b) a single supramolecular junction of $\pi-\pi$ dimers, and (c) a mechanically interlocked molecular junction.

experimental design provides two powerful methods to understand the electron generation and electron trapping processes at the MIMs−graphene interface under photoirradiation. One is the mirror-image photoswitching of redox-bistable MIMs−graphene hybrids, and the other is the nonvolatile memory effects in the single graphene sheet. Second, soft contact between molecules and the top electrode will alleviate the damage during fabrication of sandwich-architecture devices. For example, Lörtscher and co-workers reported a nondestructive top-contact technique, which directly deposits an interlayer consisting of metallic nanoparticles atop the monolayer from solution prior to the metal electrode evaporation (Figure 7g).[100] The ambient-stable devices show satisfactory charge transport properties, and the interlayer consisting of metallic nanoparticles and additive top metalization has slight influence on the electron transport. Interface engineering proves to be a promising strategy to construct the vertical tunneling devices. Duan and co-workers demonstrated that free-standing single-layer graphene can also serve as the top electrode to achieve a soft contact with the monolayer.[101−103] Vertical Au/SAM/graphene tunnel junctions are adopted to make stable molecular transistors[101,103] and redox switches.[102] These methodologies allow the possibility of large-scale fabrication of ambient-stable MSTJ devices and integrated memristors in the near future. Third, the self-assembly properties of active conducting monolayers also play a key role in realizing the mechanically and electronically robust monolayer junctions. Qiu and co-workers demonstrated the self-assembled bilayers of fullerenes functionalized with glycol ethers, which exhibit ambient stability for several weeks.[104] The use of amphiphilic molecules mimics the self-assembly behavior of the phospholipid bilayer structure in cell membranes.[105] A weak charge-transfer bonding attaches fullerene to the substrate, which ensures

https://doi.org/10.1021/acsanm.2c01880
ACS Appl. Nano Mater. 2022, 5, 13874−13886

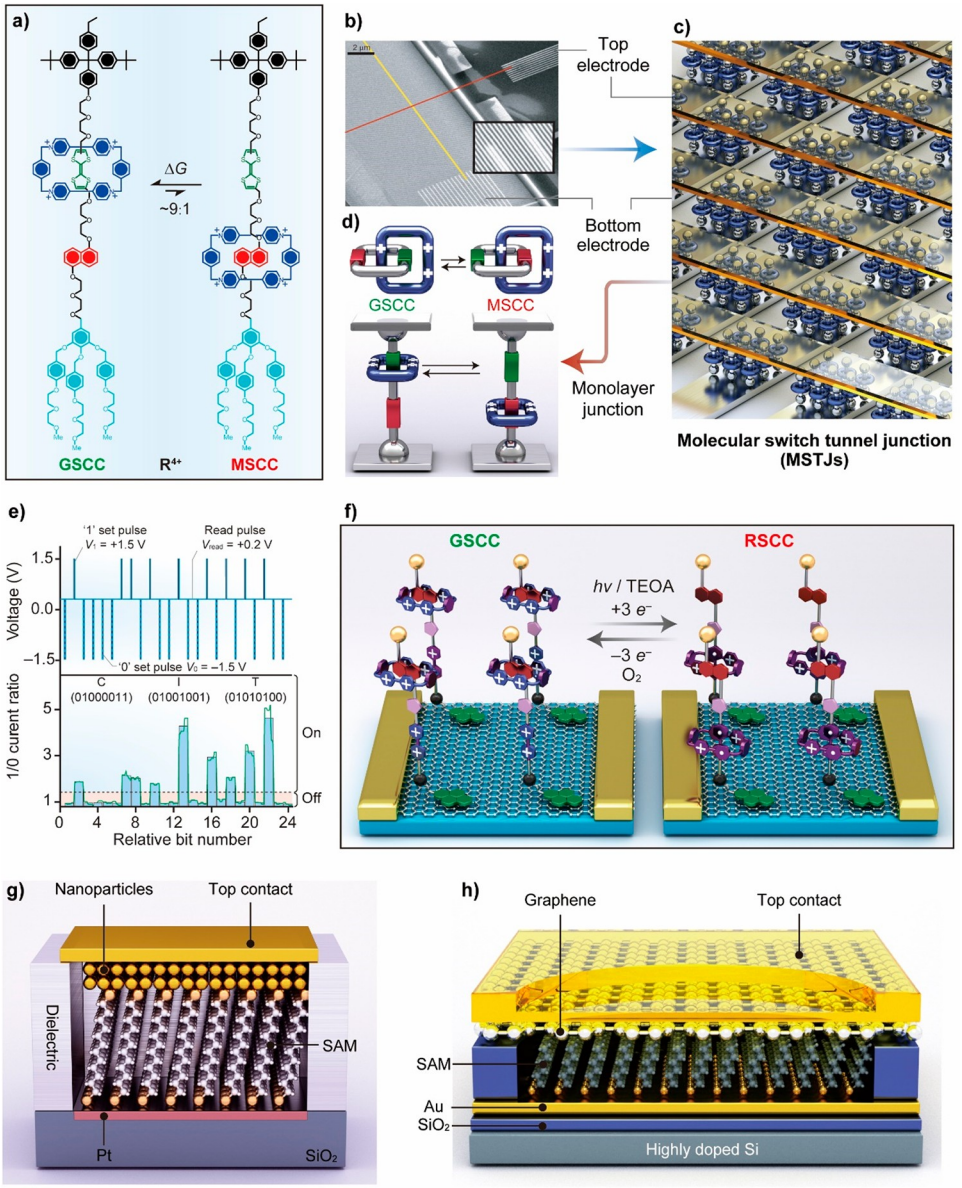

Figure 7. (a) Structural formulas of redox-induced switching of the [2]rotaxane; the counter ions are omitted for clarity. (b) High-resolution scanning electron microscope image of a random-access memory device constructed with MSTJs. (c) Schematic illustration showing the structure of integrated MSTJs. (d) Schematic illustration showing the co-conformational changes of [2]catenane (top) and [2]rotaxane (bottom). (e) The switching operation of a random-access memory molecular device by applying different pulse sequences (top) and storing ASCII information on "CIT" in binary numbers (bottom). (f) Schematic illustration showing the device structure of a [2]rotaxane monolayer adsorbed on a single-layer graphene sheet atop a Si/SiO_2 substrate. (g) Schematic illustration showing metallic nanoparticle contacts for efficient, ambient-stable vertical nanodevices. (h) Schematic illustration showing monolayer junctions with single-layer graphene as the top electrode. (a–e) Reprinted with permission from ref 13. Copyright 2021, Springer Nature Limited. (f) Reprinted with permission from ref 99. Copyright 2013, Wiley.

the uniform coverage of SAM through lateral diffusion. Meanwhile, hydrogen bonding between the glycol ether tails provides the strength of the bilayer. In another work, El Abbassi reported a lateral monolayer junction, in which a robust electronic stability was achieved by optimizing the $\pi-\pi$ interactions between neighboring molecules.[106] These works have shed light on the molecular engineering of MIMs to achieve the reproducible and controllable electronic features of MSTJs.

4. SINGLE-MOLECULE JUNCTIONS BASED ON MIMS

Compared with MSTJs, single molecular junctions based on MIMs give abundant and idiographic information about conformational changes and noncovalent interactions within individual molecules.[107,108] In addition to the improved stability of conjugated molecular conductors provided by interlocked structures during the conductivity measurements, MIMs have two other prominent effects. One effect is to suppress the intramolecular motion, and the other is to eliminate the inter(intra)molecular interactions. The host–guest interaction of MIMs provides the possibility to control or avoid these downsides in conductivity measurements. Kiguchi and co-workers demonstrated a promising method to suppress the conductance fluctuations by means of wrapping a π-conjugated molecular wire into an α-cyclodextrin macrocycle (Figure 8a).[30] The conductance histogram measured with the

https://doi.org/10.1021/acsanm.2c01880
ACS Appl. Nano Mater. 2022, 5, 13874–13886

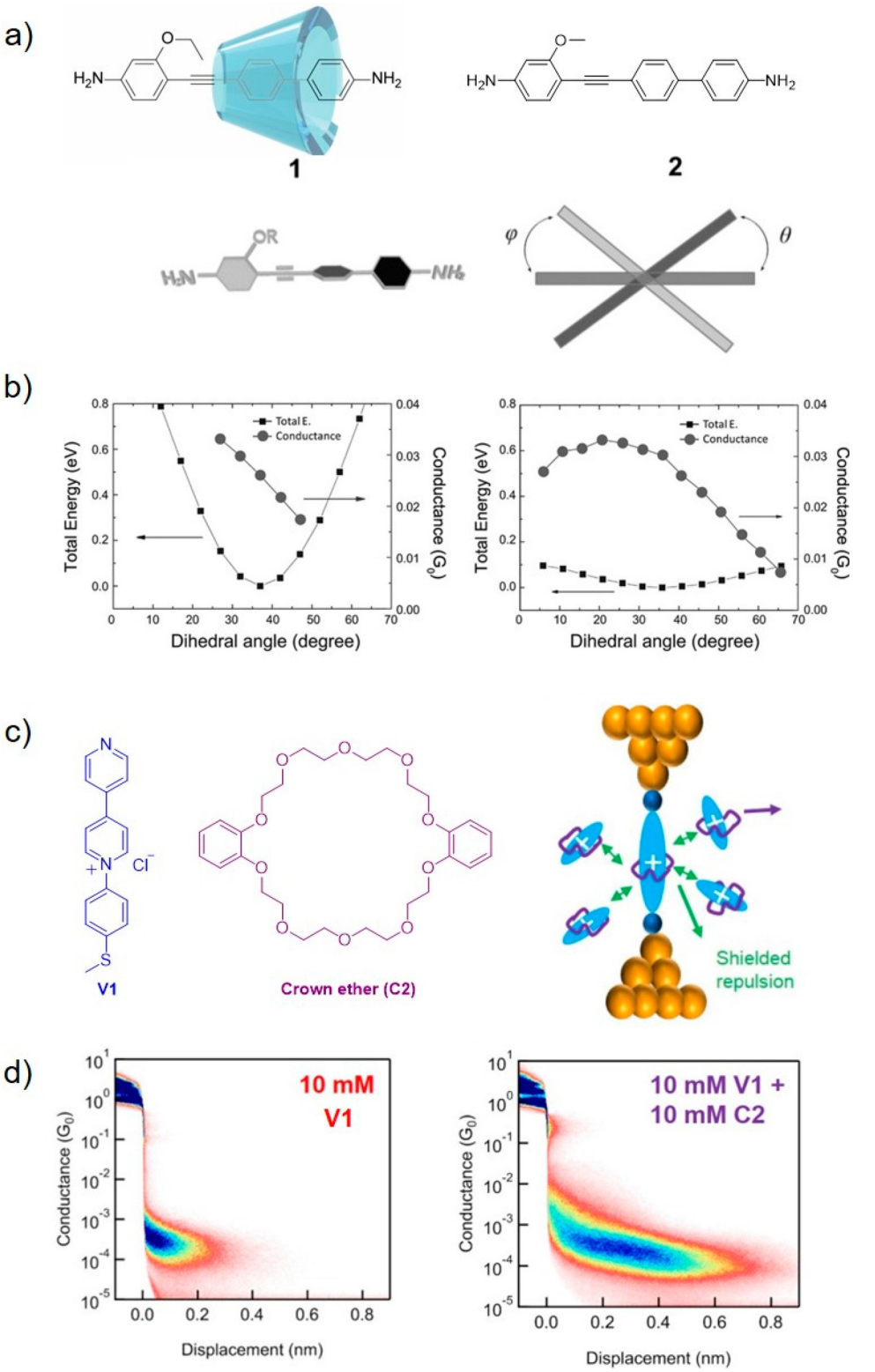

Figure 8. (a) Schematic illustration showing the shuttling and rotating of a guest molecule in an interlocked host−guest molecule. (b) The calculated conductance and total energy as a function of dihedral angles for two similar structures, i.e., a pseudorotaxane molecular junction (left) and a free dumbbell molecular junction (right). (c) Structural formulas of V1 guest molecule (left) and crown ether C2 host molecule (middle) and a schematic illustration of their host−guest supramolecular junction (right). (d) Two-dimensional conductance−distance histograms of V1 (left) and the host−guest complex (right). (a, b) Reprinted with permission from ref 30. Copyright 2012, Wiley. (c, d) Reprinted with permission from ref 109. Copyright 2020, Elsevier.

STM-BJ technique shows that the observed conductance peaks of the pseudorotaxane are sharper than those of the individual π-conjugated molecular wire (Figure 8b). In another case, Schroeder and co-workers found that the conductivity of positively charged pyridinium-based junctions shows reduced molecular displacements in high concentrations because of

https://doi.org/10.1021/acsanm.2c01880
ACS Appl. Nano Mater. 2022, 5, 13874−13886

electrostatic repulsion effects (Figure 8c).[109] However, the formation of host−guest complexes between pyridinium and the crown ether results in normal molecular displacements relevant to the length of a single pyridinium molecule (Figure 8d). These results thereby suggest that host−guest complexation screens electrostatic repulsions efficiently between cationic molecules.

MIMs have also been used to make single-molecule transistors. Heath and co-workers have utilized a three-terminal single-molecule device to investigate the charge transport in redox-switchable [2]rotaxanes.[110] Differential conductance (dI/dV) curves demonstrate a gate voltage-dependent electron conductance of the device. In the case of Borromean ring complexes, gated double-barrier tunneling junctions are fabricated using break-junction techniques.[111] In addition to the single-molecule transistor function, this device has demonstrated a rectification of conductance when the Borromean complex has anchor groups attached to the electrodes.

5. REAL-TIME PROBING OF SINGLE-MOLECULE DYNAMICS OF MIMS

Understanding dynamics at the single-molecule scale is indispensable for designing useful molecular machines.[112] The real-time dynamic motion of MIMs, i.e., shuttling, traversing, and rocking, is far from easy to be monitored by conventional techniques for the simple reason that the ensemble experiments in solution often give averaged properties.[113] Electrochemically driven single-molecule dynamics within bistable rotaxanes have been achieved by direct electrical measurements using STM platforms.[114] These molecules anchored laterally on gold surfaces have shown significantly low mobility and better assembly orientations (Figure 9a). By changing the electrode potential from 0.12 to 0.53 V, the oxidation and reduction processes of bistable [2]rotaxane take place on the surface. The dynamic motions within these surface-bound [2]rotaxanes are influenced by the interaction with the surface of Au, as well as the interaction with neighboring MIMs.

Graphene single-molecule junction techniques provide promising real-time platforms to explain intrinsic mechanisms associated with inter(intra)molecular interactions in MIMs (Figure 9b).[113,115] In a transistor-like platform,[26] conducting molecular wires with macrocyclic side units as local gates are connected covalently to the graphene electrodes at both ends. This technique enables the direct measurements of currents associated with host−guest interaction within the macrocyclic side group (Figure 9b, right).[26] When a dicationic bipyridinium motif goes through a crown ether, an irregular current signal occurs, which indicates the formation of a complexed structure. To investigate the dynamic shuttling behavior of pseudorotaxanes,[27] three functional dodecamethylene groups bearing different kind of charges on the chain ends are used to construct the molecular shuttles (Figure 9c).[27] The dodecanedioic acid group has a positive charge property, and the 1,12-dodecanediamine shows a negative charge performance, while 12-aminododecanoic acid presents an amphoteric charge behavior. Three molecular shuttles consisting of cyclodextrin and different alkylene chains with different charge characteristics show large-amplitude two-level or three-level conductance states within the time scale of a few milliseconds by performing current−time measurements. In a similar approach, real-time observation of the molecular

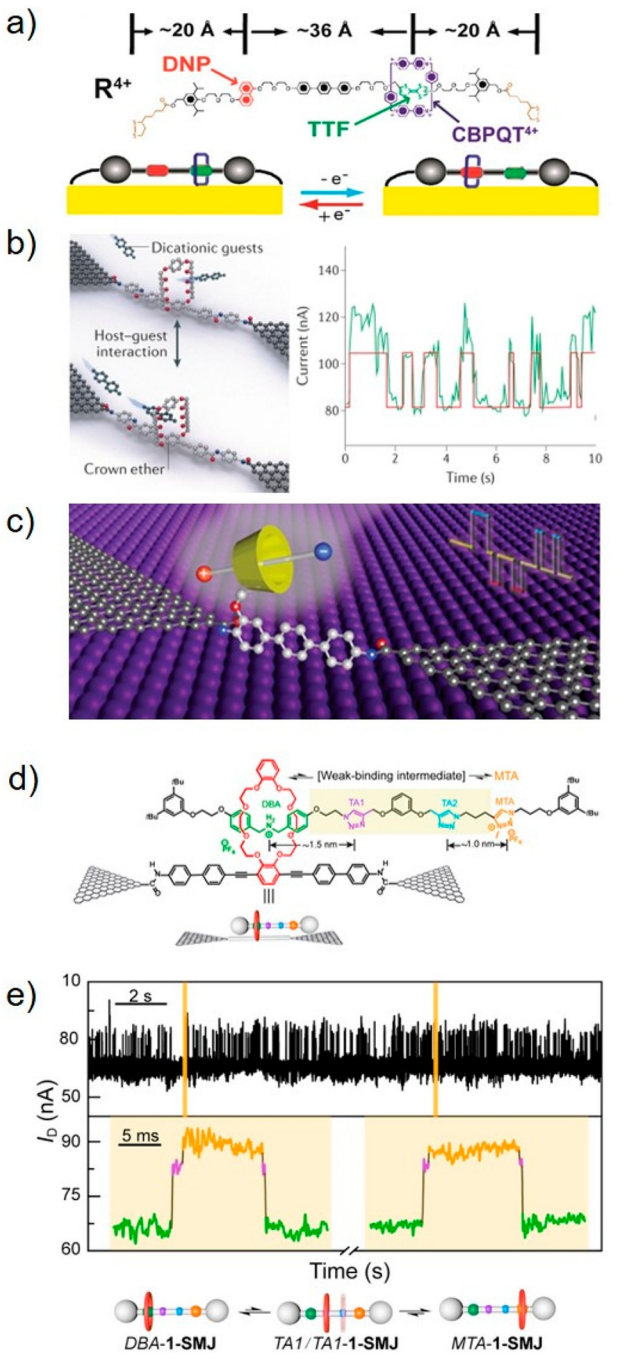

Figure 9. (a) Schematic illustration showing the structure and dynamic motion of a [2]rotaxane absorbed on the Au surface. (b) Left: schematic illustrating the different host−guest interactions between a dicationic bipyridinium molecule and a crown ether. Right: real-time current−time data with its fitting curve. (c) Schematic illustration showing the translation dynamics of a pseudorotaxane based on graphene single-molecule junctions. (d) Schematic illustrating the construction of a graphene single-molecule junction to investigate the real-time motion dynamics of a [2]rotaxane molecular shuttle. (e) Real-time current−time curves of investigated [2]rotaxane immersed in DMSO, showing the co-conformation change between two molecular recognition sites. (a) Reprinted with permission from ref 114. Copyright 2010, American Chemical Society. (b) Reprinted with permission from ref 13. Copyright 2021, Springer Nature Limited. (c) Reprinted with permission from ref 27. Copyright 2019, Wiley. (d, e) Reprinted with permission from ref 28. Copyright 2021, Elsevier.

https://doi.org/10.1021/acsanm.2c01880
ACS Appl. Nano Mater. 2022, 5, 13874−13886

dynamics of an individual rotaxane is achieved through a similar graphene SMJ technique (Figure 9d).[28] In addition to two conventional conformations, a short-lived intermediate state of co-conformations in [2]rotaxane is detected, although it is not apparent using time-average techniques, such as NMR spectroscopy (Figure 9e). These advances have illustrated how single-molecule techniques can open up new opportunities for revealing the aspects of co-conformations, translational dynamics, and operational mechanisms associated with MIMs that are hidden as averaged behavior in ensembles when using conversional techniques.

6. CONCLUSIONS AND OUTLOOK

In this Review, we summarize the structures, properties, and functions of MIMs when they are used as conductors in single-molecule devices. Compared with conventional molecular junctions, these mechanically interlocked molecular junctions (MIMJs) present attractive properties because of their interlocked structures, co-conformational flexibilities, and dynamic noncovalent interactions. There is no doubt that MIMs, with their abundant topological and structural properties, will continue to be a cornerstone in the field of molecular electronics. We bring closure to this Review by raising some potential directions worthy of exploring in MIMJs, namely (i) theoretical calculations, (ii) technical developments, and (iii) the drive toward applications.

First, MIMJs will have many of the same issues that SMJs have faced in the field of theoretical calculations. It is difficult to model or simulate the MIMs systems for the simple reason that as the molecular size scales, the accuracy of calculations or models decreases substantially. The multiple noncovalent interactions within MIMs make the theoretical simulations more complicated. Usually, the models will produce results that are several orders of magnitude different from the experimental results. To solve this issue, strong collaborations between theoretical and experimental scientists are needed to pursue a continued development of theoretical methods for MIMJs.

Second, scientists and engineers still have to solve many challenges by improving the structures and functions of MIMJs to achieve stable performance and valuable applications. The detailed measurements and analyses on the enthalpic and entropic values in different MIMJs are still difficult. Quantitative determination on the kinetic and dynamic behavior of co-conformational changes of MIMs at the single-molecule level is still on an uneven road, because the connection, coupling, and interaction of molecules and electrodes are not very stable. Furthermore, although the AFM technique is a fairly useful tool to measure subtle force changes and offers detailed information on intermolecular interactions of MIMs, several other problems, i.e., the challenge of integrating force with conductance measurements and the damage to the molecules during the pulling and stretching processes, may hinder its further development. Other multiparameter-integrated measuring platforms are necessary to investigate the essential feature of the subtle dynamic motions and structural changes of MIMs at the single-molecule and even single-bond level.

Third, MIMJs are the perfect combination between solid-state molecular nanodevices and mechanically interlocked structures. In the development of MIMJs, deep and comprehensive collaborations are necessary between scientists in different fields including mechanochemistry, nanomaterials, nanotechnology, biophysics, and even pharmacology to achieve better investigation and understanding of MIMJs in real and practical applications. Technical improvements, including combination with synthetic chemistry, nanotechnology, and machine learning, are pivotal in optimizing the performance as well as developing new functions of MIMJs. Because of the continuous dedication to molecular devices based on MIMs, it is firmly believed that nanodevices of MIMs and molecular machines will be promising candidates for integrated molecular circuits beyond Moore's Law.

AUTHOR INFORMATION

Corresponding Author

Hongliang Chen − *Stoddart Institute of Molecular Science, Department of Chemistry, Zhejiang University, Hangzhou 310027, China; ZJU-Hangzhou Global Scientific and Technological Innovation Center, Hangzhou 311215, China;* orcid.org/0000-0002-4442-7984; Email: hongliang.chen@zju.edu.cn

Author

Chaoqing Yang − *Stoddart Institute of Molecular Science, Department of Chemistry, Zhejiang University, Hangzhou 310027, China; ZJU-Hangzhou Global Scientific and Technological Innovation Center, Hangzhou 311215, China*

Complete contact information is available at: https://pubs.acs.org/10.1021/acsanm.2c01880

Notes

The authors declare no competing financial interest.

ACKNOWLEDGMENTS

The authors thank Zhejiang University (ZJU) for continued support of this research, which was also funded by the Starry Night Science Fund of Zhejiang University Shanghai Institute for Advanced Study, grant no. SN-ZJU-SIAS-006. The authors also thank Shanghai ShengSheng Logistics for financial support.

REFERENCES

(1) Sauvage, J. P. From chemical topology to molecular machines (Nobel Lecture). *Angew. Chem., Int. Ed.* **2017**, *56*, 11080−11093.

(2) Stoddart, J. F. Mechanically interlocked molecules (MIMs)—molecular shuttles, switches, and machines (Nobel Lecture). *Angew. Chem., Int. Ed.* **2017**, *56*, 11094−11125.

(3) Feringa, B. L. The art of building small: from molecular switches to motors (Nobel Lecture). *Angew. Chem., Int. Ed.* **2017**, *56*, 11060−11078.

(4) Elizarov, A. M.; Chiu, S.-H.; Stoddart, J. F. An acid−base switchable [2]rotaxane. *J. Org. Chem.* **2002**, *67*, 9175−9181.

(5) Cheng, C.; McGonigal, P. R.; Schneebeli, S. T.; Li, H.; Vermeulen, N. A.; Ke, C.; Stoddart, J. F. An artificial molecular pump. *Nat. Nanotechnol* **2015**, *10*, 547−553.

(6) Koumura, N.; Zijlstra, R. W.; van Delden, R. A.; Harada, N.; Feringa, B. L. Light-driven monodirectional molecular rotor. *Nature* **1999**, *401*, 152−155.

(7) Saywell, A.; Bakker, A.; Mielke, J.; Kumagai, T.; Wolf, M.; García-López, V.; Chiang, P.-T.; Tour, J. M.; Grill, L. Light-induced translation of motorized molecules on a surface. *ACS Nano* **2016**, *10*, 10945−10952.

(8) Bruns, C. J.; Stoddart, J. F. *The nature of the mechanical bond: from molecules to machines*; Wiley, 2016.

(9) Deng, Y.; Lai, S. K.-M.; Kong, L.; Au-Yeung, H. Y. Fine-tuning of the optical output in a dual responsive catenane switch. *Chem. Commun.* **2021**, *57*, 2931−2934.

(10) Bissell, R. A.; Córdova, E.; Kaifer, A. E.; Stoddart, J. F. A chemically and electrochemically switchable molecular shuttle. *Nature* **1994**, *369*, 133−137.
(11) Chang, J.-C.; Tseng, S.-H.; Lai, C.-C.; Liu, Y.-H.; Peng, S.-M.; Chiu, S.-H. Mechanically interlocked daisy-chain-like structures as multidimensional molecular muscles. *Nat. Chem.* **2017**, *9*, 128−134.
(12) Coskun, A.; Spruell, J. M.; Barin, G.; Dichtel, W. R.; Flood, A. H.; Botros, Y. Y.; Stoddart, J. F. High hopes: can molecular electronics realise its potential? *Chem. Soc. Rev.* **2012**, *41*, 4827−4859.
(13) Chen, H.; Stoddart, J. F. From molecular to supramolecular electronics. *Nat. Rev. Mater.* **2021**, *6*, 804−828.
(14) Frisenda, R.; Janssen, V. A.; Grozema, F. C.; Van Der Zant, H. S.; Renaud, N. Mechanically controlled quantum interference in individual π-stacked dimers. *Nat. Chem.* **2016**, *8*, 1099−1104.
(15) Huang, S.; He, J.; Chang, S.; Zhang, P.; Liang, F.; Li, S.; Tuchband, M.; Fuhrmann, A.; Ros, R.; Lindsay, S. Identifying single bases in a DNA oligomer with electron tunnelling. *Nat. Nanotechnol.* **2010**, *5*, 868−873.
(16) Wen, H.; Li, W.; Chen, J.; He, G.; Li, L.; Olson, M. A.; Sue, A. C.-H.; Stoddart, J. F.; Guo, X. Complex formation dynamics in a single-molecule electronic device. *Sci. Adv.* **2016**, *2*, e1601113.
(17) Chen, H.; Brasiliense, V.; Mo, J.; Zhang, L.; Jiao, Y.; Chen, Z.; Jones, L. O.; He, G.; Guo, Q.-H.; Chen, X.-Y.; Song, B.; Schatz, G. C.; Stoddart, J. F. Single-molecule charge transport through positively charged electrostatic anchors. *J. Am. Chem. Soc.* **2021**, *143*, 2886−2895.
(18) Chen, H.; Jiang, F.; Hu, C.; Jiao, Y.; Chen, S.; Qiu, Y.; Zhou, P.; Zhang, L.; Cai, K.; Song, B.; Chen, X.-Y.; Zhao, X.; Wasielewski, M. R.; Guo, H.; Hong, W.; Stoddart, J. F. Electron-catalyzed dehydrogenation in a single-molecule junction. *J. Am. Chem. Soc.* **2021**, *143*, 8476−8487.
(19) Chen, H.; Zheng, H.; Hu, C.; Cai, K.; Jiao, Y.; Zhang, L.; Jiang, F.; Roy, I.; Qiu, Y.; Shen, D.; Feng, Y.; Alsubaie, F. M.; Guo, H.; Hong, W.; Stoddart, J. F. Giant conductance enhancement of intramolecular circuits through interchannel gating. *Matter* **2020**, *2*, 378−389.
(20) Chen, H.; Hou, S.; Wu, Q.; Jiang, F.; Zhou, P.; Zhang, L.; Jiao, Y.; Song, B.; Guo, Q.-H.; Chen, X.-Y.; Hong, W.; Lambert, C. J.; Stoddart, J. F. Promotion and suppression of single-molecule conductance by quantum interference in macrocyclic circuits. *Matter* **2021**, *4*, 3662−3676.
(21) Sluysmans, D.; Lussis, P.; Fustin, C.-A.; Bertocco, A.; Leigh, D. A.; Duwez, A.-S. Real-time fluctuations in single-molecule rotaxane experiments reveal an intermediate weak binding state during shuttling. *J. Am. Chem. Soc.* **2021**, *143*, 2348−2352.
(22) Sluysmans, D.; Hubert, S.; Bruns, C. J.; Zhu, Z.; Stoddart, J. F.; Duwez, A.-S. Synthetic oligorotaxanes exert high forces when folding under mechanical load. *Nat. Nanotechnol.* **2018**, *13*, 209−213.
(23) Sluysmans, D.; Devaux, F.; Bruns, C. J.; Stoddart, J. F.; Duwez, A.-S. Dynamic force spectroscopy of synthetic oligorotaxane foldamers. *Proc. Natl. Acad. Sci. U.S.A.* **2018**, *115*, 9362−9366.
(24) Van Quaethem, A.; Lussis, P.; Leigh, D. A.; Duwez, A.-S.; Fustin, C.-A. Probing the mobility of catenane rings in single molecules. *Chem. Sci.* **2014**, *5*, 1449−1452.
(25) Lussis, P.; Svaldo-Lanero, T.; Bertocco, A.; Fustin, C.-A.; Leigh, D. A.; Duwez, A.-S. A single synthetic small molecule that generates force against a load. *Nat. Nanotechnol.* **2011**, *6*, 553−557.
(26) Wen, H.; Li, W.; Chen, J.; He, G.; Li, L.; Olson, M. A.; Sue, A. C.-H.; Stoddart, J. F.; Guo, X. Complex formation dynamics in a single-molecule electronic device. *Sci. Adv.* **2016**, *2*, e1601113.
(27) Zhou, C.; Li, X.; Masai, H.; Liu, Z.; Lin, Y.; Tamaki, T.; Terao, J.; Yang, J.; Guo, X. Revealing charge-and temperature-dependent movement dynamics and mechanism of individual molecular machines. *Small Methods* **2019**, *3*, 1900464.
(28) Chen, S.; Su, D.; Jia, C.; Li, Y.; Li, X.; Guo, X.; Leigh, D. A.; Zhang, L. Real-time observation of the dynamics of an individual rotaxane molecular shuttle using a single-molecule junction. *Chem* **2022**, *8*, 243−252.
(29) Liu, Z.; Li, X.; Masai, H.; Huang, X.; Tsuda, S.; Terao, J.; Yang, J.; Guo, X. A single-molecule electrical approach for amino acid detection and chirality recognition. *Sci. Adv.* **2021**, *7*, eabe4365.
(30) Kiguchi, M.; Nakashima, S.; Tada, T.; Watanabe, S.; Tsuda, S.; Tsuji, Y.; Terao, J. Single-molecule conductance of π-conjugated rotaxane: new method for measuring stipulated electric conductance of π-conjugated molecular wire using STM break junction. *Small* **2012**, *8*, 726−730.
(31) Green, J. E.; Wook Choi, J.; Boukai, A.; Bunimovich, Y.; Johnston-Halperin, E.; DeIonno, E.; Luo, Y.; Sheriff, B. A.; Xu, K.; Shik Shin, Y.; et al. A 160-kilobit molecular electronic memory patterned at 10^{11} bits per square centimetre. *Nature* **2007**, *445*, 414−417.
(32) Anelli, P. L.; Ashton, P. R.; Ballardini, R.; Balzani, V.; Delgado, M.; Gandolfi, M. T.; Goodnow, T. T.; Kaifer, A. E.; Philp, D. Molecular meccano. 1. [2] Rotaxanes and a [2] catenane made to order. *J. Am. Chem. Soc.* **1992**, *114*, 193−218.
(33) Brown, C. L.; Jonas, U.; Preece, J. A.; Ringsdorf, H.; Seitz, M.; Stoddart, J. F. Introduction of [2] catenanes into Langmuir films and Langmuir−Blodgett multilayers. A possible strategy for molecular information storage materials. *Langmuir* **2000**, *16*, 1924−1930.
(34) Asakawa, M.; Ashton, P. R.; Balzani, V.; Credi, A.; Hamers, C.; Mattersteig, G.; Montalti, M.; Shipway, A. N.; Spencer, N.; Stoddart, J. F.; et al. A chemically and electrochemically switchable [2] catenane incorporating a tetrathiafulvalene unit. *Angew. Chem., Int. Ed.* **1998**, *37*, 333−337.
(35) Balzani, V.; Credi, A.; Mattersteig, G.; Matthews, O. A.; Raymo, F. M.; Stoddart, J. F.; Venturi, M.; White, A. J.; Williams, D. J. Switching of pseudorotaxanes and catenanes incorporating a tetrathiafulvalene unit by redox and chemical inputs. *J. Org. Chem.* **2000**, *65*, 1924−1936.
(36) Asakawa, M.; Higuchi, M.; Mattersteig, G.; Nakamura, T.; Pease, A. R.; Raymo, F. M.; Shimizu, T.; Stoddart, J. F. Current/voltage characteristics of monolayers of redox-switchable [2] catenanes on gold. *Adv. Mater.* **2000**, *12*, 1099−1102.
(37) Collier, C. P.; Mattersteig, G.; Wong, E. W.; Luo, Y.; Beverly, K.; Sampaio, J.; Raymo, F. M.; Stoddart, J. F.; Heath, J. R. A [2]catenane-based solid state electronically reconfigurable switch. *Science* **2000**, *289*, 1172−1175.
(38) Jeppesen, J. O.; Perkins, J.; Becher, J.; Stoddart, J. F. Slow shuttling in an amphiphilic bistable [2] rotaxane incorporating a tetrathiafulvalene unit. *Angew. Chem., Int. Ed.* **2001**, *113*, 1256−1261.
(39) Ma, X.; Tian, H. Bright functional rotaxanes. *Chem. Soc. Rev.* **2010**, *39*, 70−80.
(40) Au-Yeung, H. Y.; Deng, Y. Distinctive features and challenges in catenane chemistry. *Chem. Sci.* **2022**, *13*, 3315−3334.
(41) Goujon, A.; Moulin, E.; Fuks, G.; Giuseppone, N. [c2] Daisy chain rotaxanes as molecular muscles. *CCS Chem.* **2019**, *1*, 83−96.
(42) Coskun, A.; Banaszak, M.; Astumian, R. D.; Stoddart, J. F.; Grzybowski, B. A. Great expectations: can artificial molecular machines deliver on their promise? *Chem. Soc. Rev.* **2012**, *41*, 19−30.
(43) Pearce, N.; Tarnowska, M.; Andersen, N. J.; Wahrhaftig-Lewis, A.; Pilgrim, B. S.; Champness, N. R. Mechanically interlocked molecular handcuffs. *Chem. Sci.* **2022**, *13*, 3915−3941.
(44) Guo, Q.-H.; Jiao, Y.; Feng, Y.; Stoddart, J. F. The rise and promise of molecular nanotopology. *CCS Chem.* **2021**, *3*, 1542−1572.
(45) Xue, M.; Yang, Y.; Chi, X.; Yan, X.; Huang, F. Development of Pseudorotaxanes and Rotaxanes: From synthesis to stimuli-responsive motions to applications. *Chem. Rev.* **2015**, *115*, 7398−7501.
(46) Rotzler, J.; Mayor, M. Molecular daisy chains. *Chem. Soc. Rev.* **2013**, *42*, 44−62.
(47) Segawa, Y.; Kuwayama, M.; Hijikata, Y.; Fushimi, M.; Nishihara, T.; Pirillo, J.; Shirasaki, J.; Kubota, N.; Itami, K. Topological molecular nanocarbons: all-benzene catenane and trefoil knot. *Science* **2019**, *365*, 272−276.
(48) Chichak, K. S.; Cantrill, S. J.; Pease, A. R.; Chiu, S.-H.; Cave, G. W.; Atwood, J. L.; Stoddart, J. F. Molecular borromean rings. *Science* **2004**, *304*, 1308−1312.

https://doi.org/10.1021/acsanm.2c01880
ACS Appl. Nano Mater. 2022, 5, 13874−13886

(49) Amabilino, D. B.; Ashton, P. R.; Reder, A. S.; Spencer, N.; Stoddart, J. F. Olympiadane. *Angew. Chem., Int. Ed.* **1994**, *33*, 1286−1290.
(50) Moulin, E.; Faour, L.; Carmona-Vargas, C. C.; Giuseppone, N. From molecular machines to stimuli-responsive materials. *Adv. Mater.* **2020**, *32*, 1906036.
(51) Dattler, D.; Fuks, G.; Heiser, J.; Moulin, E.; Perrot, A.; Yao, X.; Giuseppone, N. Design of collective motions from synthetic molecular switches, rotors, and motors. *Chem. Rev.* **2020**, *120*, 310−433.
(52) Trabolsi, A.; Khashab, N.; Fahrenbach, A. C.; Friedman, D. C.; Colvin, M. T.; Cotí, K. K.; Benítez, D.; Tkatchouk, E.; Olsen, J.-C.; Belowich, M. E.; Carmielli, R.; Khatib, H. A.; Goddard, W. A., III; Wasielewski, M. R.; Stoddart, J. F. Radically enhanced molecular recognition. *Nat. Chem.* **2010**, *2*, 42−49.
(53) Pezzato, C.; Nguyen, M. T.; Kim, D. J.; Anamimoghadam, O.; Mosca, L.; Stoddart, J. F. Controlling dual molecular pumps electrochemically. *Angew. Chem., Int. Ed.* **2018**, *57*, 9325−9329.
(54) Qiu, Y.; Song, B.; Pezzato, C.; Shen, D.; Liu, W.; Zhang, L.; Feng, Y.; Guo, Q.-H.; Cai, K.; Li, W.; Chen, H.; Nguyen, M. T.; Shi, Y.; Cheng, C.; Astumian, R. D.; Li, X.; Stoddart, J. F. A precise polyrotaxane synthesizer. *Science* **2020**, *368*, 1247−1253.
(55) Jiao, Y.; Qiu, Y.; Zhang, L.; Liu, W. G.; Mao, H.; Chen, H.; Feng, Y.; Cai, K.; Shen, D.; Song, B.; Chen, X. Y.; Li, X.; Zhao, X.; Young, R. M.; Stern, C. L.; Wasielewski, M. R.; Astumian, R. D.; Goddard, W. A., III; Stoddart, J. F. Electron-catalysed molecular recognition. *Nature* **2022**, *603*, 265−270.
(56) Li, H.; Cheng, C.; McGonigal, P. R.; Fahrenbach, A. C.; Frasconi, M.; Liu, W.-G.; Zhu, Z.; Zhao, Y.; Ke, C.; Lei, J.; Young, R. M.; Dyar, S. M.; Co, D. T.; Yang, Y.-W.; Botros, Y. Y.; Goddard, W. A., III; Wasielewski, M. R.; Astumian, R. D.; Stoddart, J. F. Relative unidirectional translation in an artificial molecular assembly fueled by light. *J. Am. Chem. Soc.* **2013**, *135*, 18609−18620.
(57) Balzani, V.; Clemente-León, M.; Credi, A.; Ferrer, B.; Venturi, M.; Flood, A. H.; Stoddart, J. F. Autonomous artificial nanomotor powered by sunlight. *Proc. Natl. Acad. Sci. U.S.A.* **2006**, *103*, 1178−1183.
(58) Anelli, P. L.; Spencer, N.; Stoddart, J. F. A molecular shuttle. *J. Am. Chem. Soc.* **1991**, *113*, 5131−5133.
(59) Schröder, H. V.; Mekic, A.; Hupatz, H.; Sobottka, S.; Witte, F.; Urner, L. H.; Gaedke, M.; Pagel, K.; Sarkar, B.; Paulus, B.; Schalley, C. A. Switchable synchronisation of pirouetting motions in a redox-active [3]rotaxane. *Nanoscale* **2018**, *10*, 21425−21433.
(60) Ashton, P. R.; Goodnow, T. T.; Kaifer, A. E.; Reddington, M. V.; Slawin, A. M. Z.; Spencer, N.; Stoddart, J. F.; Vicent, C.; Williams, D. J. A [2]catenane made to order. *Angew. Chem., Int. Ed.* **1989**, *28*, 1396−1399.
(61) Tseng, H.-R.; Vignon, S. A.; Stoddart, J. F. Toward chemically controlled nanoscale molecular machinery. *Angew. Chem., Int. Ed.* **2003**, *42*, 1491−1495.
(62) Jiang, G.; Chen, Y.; Ji, Y.; Chen, W.; Zhang, X.; Zheng, Y. Strong polarity asymmetry and abnormal mechanical electroresistance effect in the organic monolayer tunnel junction. *ACS Appl. Electron. Mater.* **2019**, *1*, 1084−1090.
(63) Shao, J.; Zhu, W.; Zhang, X.; Zheng, Y. Molecular rotors with designed polar rotating groups possess mechanics-controllable wide-range rotational speed. *NPJ. Comput. Mater.* **2020**, *6*, 185.
(64) Deng, W.-Q.; Muller, R. P.; Goddard, W. A., III Mechanism of the Stoddart−Heath bistable rotaxane molecular switch. *J. Am. Chem. Soc.* **2004**, *126*, 13562−13563.
(65) Dichtel, W. R.; Miljanić, O. Š.; Spruell, J. M.; Heath, J. R.; Stoddart, J. F. Efficient templated synthesis of donor−acceptor rotaxanes using click chemistry. *J. Am. Chem. Soc.* **2006**, *128*, 10388−10390.
(66) Bazargan, G.; Sohlberg, K. Advances in modelling switchable mechanically interlocked molecular architectures. *Int. Rev. Phys. Chem.* **2018**, *37*, 1−82.
(67) Trabolsi, A.; Fahrenbach, A. C.; Dey, S. K.; Share, A. I.; Friedman, D. C.; Basu, S.; Gasa, T. B.; Khashab, N. M.; Saha, S.; Aprahamian, I.; et al. A tristable [2]pseudo[2]rotaxane. *Chem. Commun.* **2010**, *46*, 871−873.
(68) Avellini, T.; Li, H.; Coskun, A.; Barin, G.; Trabolsi, A.; Basuray, A. N.; Dey, S. K.; Credi, A.; Silvi, S.; Stoddart, J. F.; Venturi, M. Photoinduced memory effect in a redox controllable bistable mechanical molecular switch. *Angew. Chem., Int. Ed.* **2012**, *124*, 1643−1647.
(69) Frampton, M. J.; Anderson, H. L. Insulated molecular wires. *Angew. Chem., Int. Ed.* **2007**, *46*, 1028−1064.
(70) Ajayaghosh, A.; Praveen, V. K.; Vijayakumar, C.; George, S. J. J. A. C. Molecular wire encapsulated into π organogels: efficient supramolecular light-harvesting antennae with color-tunable emission. *Angew. Chem., Int. Ed.* **2007**, *119*, 6376−6381.
(71) Chen, X.; Kretz, B.; Adoah, F.; Nickle, C.; Chi, X.; Yu, X.; Del Barco, E.; Thompson, D.; Egger, D. A.; Nijhuis, C. A. A single atom change turns insulating saturated wires into molecular conductors. *Nat. Commun.* **2021**, *12*, 3432.
(72) Buston, J. E.; Marken, F.; Anderson, H. L. Enhanced chemical reversibility of redox processes in cyanine dye rotaxanes. *Chem. Commun.* **2001**, 1046−1047.
(73) Taylor, P. N.; Hagan, A. J.; Anderson, H. L. Hindered fluorescence quenching in an insulated molecular wire. *Org. Biomol. Chem.* **2003**, *1*, 3851−3856.
(74) Taylor, P. N.; O'Connell, M. J.; McNeill, L. A.; Hall, M. J.; Aplin, R. T.; Anderson, H. L. Insulated molecular wires: synthesis of conjugated polyrotaxanes by Suzuki coupling in water. *Angew. Chem., Int. Ed.* **2000**, *39*, 3456−3460.
(75) Cacialli, F.; Wilson, J. S.; Michels, J. J.; Daniel, C.; Silva, C.; Friend, R. H.; Severin, N.; Samorì, P.; Rabe, J. P.; O'Connell, M. J.; et al. Cyclodextrin-threaded conjugated polyrotaxanes as insulated molecular wires with reduced interstrand interactions. *Nat. Mater.* **2002**, *1*, 160−164.
(76) Liu, Q.; Yan, K.; Chen, J.; Xia, M.; Li, M.; Liu, K.; Wang, D.; Wu, C.; Xie, Y. Recent advances in novel aerogels through the hybrid aggregation of inorganic nanomaterials and polymeric fibers for thermal insulation. *Aggregate* **2021**, *2*, e30.
(77) Milan, D. C.; Krempe, M.; Ismael, A. K.; Movsisyan, L. D.; Franz, M.; Grace, I.; Brooke, R. J.; Schwarzacher, W.; Higgins, S. J.; Anderson, H. L.; Lambert, C. J.; Tykwinski, R. R.; Nichols, R. J. The single-molecule electrical conductance of a rotaxane-hexayne supramolecular assembly. *Nanoscale* **2017**, *9*, 355−361.
(78) Cao, Y.; Dong, S.; Liu, S.; He, L.; Gan, L.; Yu, X.; Steigerwald, M. L.; Wu, X.; Liu, Z.; Guo, X. Building high-throughput molecular junctions using indented graphene point contacts. *Angew. Chem., Int. Ed.* **2012**, *124*, 12394−12398.
(79) Guo, X.; Small, J. P.; Klare, J. E.; Wang, Y.; Purewal, M. S.; Tam, I. W.; Hong, B. H.; Caldwell, R.; Huang, L.; O'brien, S.; et al. Covalently bridging gaps in single-walled carbon nanotubes with conducting molecules. *Science* **2006**, *311*, 356−359.
(80) Tang, W.; Jiang, T.; Fan, F. R.; Yu, A. F.; Zhang, C.; Cao, X.; Wang, Z. L. Liquid-metal electrode for high-performance triboelectric nanogenerator at an instantaneous energy conversion efficiency of 70.6%. *Adv. Funct. Mater.* **2015**, *25*, 3718−3725.
(81) Arroyo, C. R.; Leary, E.; Castellanos-Gómez, A.; Rubio-Bollinger, G.; Gonzalez, M. T.; Agraït, N. Influence of binding groups on molecular junction formation. *J. Am. Chem. Soc.* **2011**, *133*, 14313−14319.
(82) Venkataraman, L.; Klare, J. E.; Tam, I. W.; Nuckolls, C.; Hybertsen, M. S.; Steigerwald, M. L. Single-molecule circuits with well-defined molecular conductance. *Nano Lett.* **2006**, *6*, 458−462.
(83) Chen, H.; Brasiliense, V.; Mo, J.; Zhang, L.; Jiao, Y.; Chen, Z.; Jones, L. O.; He, G.; Guo, Q.-H.; Chen, X.-Y.; et al. Single-molecule charge transport through positively charged electrostatic anchors. *J. Am. Chem. Soc.* **2021**, *143*, 2886−2895.
(84) Kim, Y.; Song, H. Noise spectroscopy of molecular electronic junctions. *Appl. Phys. Rev.* **2021**, *8*, 011303.
(85) Emberly, E. G.; Kirczenow, G. Models of electron transport through organic molecular monolayers self-assembled on nanoscale metallic contacts. *Phys. Rev. B* **2001**, *64*, 235412.

https://doi.org/10.1021/acsanm.2c01880
ACS Appl. Nano Mater. 2022, 5, 13874−13886

(86) Wu, S.; González, M. T.; Huber, R.; Grunder, S.; Mayor, M.; Schönenberger, C.; Calame, M. Molecular junctions based on aromatic coupling. *Nat. Nanotechnol* **2008**, *3*, 569−574.
(87) Li, X.; Wu, Q.; Bai, J.; Hou, S.; Jiang, W.; Tang, C.; Song, H.; Huang, X.; Zheng, J.; Yang, Y.; et al. Structure-independent conductance of thiophene-based single-stacking junctions. *Angew. Chem., Int. Ed.* **2020**, *59*, 3280−3286.
(88) Frisenda, R.; Janssen, V. A. E. C.; Grozema, F. C.; van der Zant, H. S. J.; Renaud, N. Mechanically controlled quantum interference in individual π-stacked dimers. *Nat. Chem.* **2016**, *8*, 1099−1104.
(89) Caneva, S.; Gehring, P.; García-Suárez, V. M.; García-Fuente, A.; Stefani, D.; Olavarria-Contreras, I. J.; Ferrer, J.; Dekker, C.; van der Zant, H. S. J. Mechanically controlled quantum interference in graphene break junctions. *Nat. Nanotechnol.* **2018**, *13*, 1126−1131.
(90) Tang, Y.; Zhou, Y.; Zhou, D.; Chen, Y.; Xiao, Z.; Shi, J.; Liu, J.; Hong, W. Electric field-induced assembly in single-stacking terphenyl junctions. *J. Am. Chem. Soc.* **2020**, *142*, 19101−19109.
(91) Luo, Y.; Collier, C. P.; Jeppesen, J. O.; Nielsen, K. A.; DeIonno, E.; Ho, G.; Perkins, J.; Tseng, H.-R.; Yamamoto, T.; Stoddart, J. F.; Heath, J. R. Two-dimensional molecular electronics circuits. *ChemPhysChem* **2002**, *3*, 519−525.
(92) Beckman, R.; Beverly, K.; Boukai, A.; Bunimovich, Y.; Choi, J. W.; DeIonno, E.; Green, J.; Johnston-Halperin, E.; Luo, Y.; Sheriff, B.; Stoddart, J. F.; Heath, J. R. Molecular mechanics and molecular electronics. *Faraday Discuss.* **2006**, *131*, 9−22.
(93) Flood, A. H.; Wong, E. W.; Stoddart, J. F. Models of charge transport and transfer in molecular switch tunnel junctions of bistable catenanes and rotaxanes. *Chem. Phys.* **2006**, *324*, 280−290.
(94) Schwartz, D. K. Langmuir-Blodgett film structure. *Small Methods* **1997**, *27*, 245−334.
(95) Jang, S. S.; Jang, Y. H.; Kim, Y.-H.; Goddard, W. A., III; Flood, A. H.; Laursen, B. W.; Tseng, H.-R.; Stoddart, J. F.; Jeppesen, J. O.; Choi, J. W.; et al. Structures and properties of self-assembled monolayers of bistable [2] rotaxanes on Au (111) surfaces from molecular dynamics simulations validated with experiment. *J. Am. Chem. Soc.* **2005**, *127*, 1563−1575.
(96) Stewart, D.; Ohlberg, D.; Beck, P.; Chen, Y.; Williams, R. S.; Jeppesen, J. O.; Nielsen, K.; Stoddart, J. F. Molecule-independent electrical switching in Pt/organic monolayer/Ti devices. *Nano Lett.* **2004**, *4*, 133−136.
(97) Chen, Y.; Ohlberg, D. A.; Li, X.; Stewart, D. R.; Stanley Williams, R.; Jeppesen, J. O.; Nielsen, K. A.; Stoddart, J. F.; Olynick, D. L.; Anderson, E. Nanoscale molecular-switch devices fabricated by imprint lithography. *Appl. Phys. Lett.* **2003**, *82*, 1610−1612.
(98) Talham, D. R. Conducting and magnetic Langmuir−Blodgett films. *Chem. Rev.* **2004**, *104*, 5479−5502.
(99) Jia, C.; Li, H.; Jiang, J.; Wang, J.; Chen, H.; Cao, D.; Stoddart, J. F.; Guo, X. Interface-engineered bistable [2rotaxane-graphene hybrids with logic capabilities. *Adv. Mater.* **2013**, *25*, 6752−6759.
(100) Puebla-Hellmann, G.; Venkatesan, K.; Mayor, M.; Lörtscher, E. Metallic nanoparticle contacts for high-yield, ambient-stable molecular-monolayer devices. *Nature* **2018**, *559*, 232−235.
(101) Famili, M.; Jia, C.; Liu, X.; Wang, P.; Grace, I. M.; Guo, J.; Liu, Y.; Feng, Z.; Wang, Y.; Zhao, Z.; et al. Self-assembled molecular-electronic films controlled by room temperature quantum interference. *Chem* **2019**, *5*, 474−484.
(102) Jia, C.; Grace, I. M.; Wang, P.; Almeshal, A.; Huang, Z.; Wang, Y.; Chen, P.; Wang, L.; Zhou, J.; Feng, Z.; et al. Redox control of charge transport in vertical ferrocene molecular tunnel junctions. *Chem* **2020**, *6*, 1172−1182.
(103) Jia, C.; Famili, M.; Carlotti, M.; Liu, Y.; Wang, P.; Grace, I. M.; Feng, Z.; Wang, Y.; Zhao, Z.; Ding, M.; et al. Quantum interference mediated vertical molecular tunneling transistors. *Sci. Adv.* **2018**, *4*, eaat8237.
(104) Qiu, X.; Ivasyshyn, V.; Qiu, L.; Enache, M.; Dong, J.; Rousseva, S.; Portale, G.; Stöhr, M.; Hummelen, J. C.; Chiechi, R. C. Thiol-free self-assembled oligoethylene glycols enable robust air-stable molecular electronics. *Nat. Mater.* **2020**, *19*, 330−337.
(105) Chen, H.; Li, M.; Lu, Z.; Wang, X.; Yang, J.; Wang, Z.; Zhang, F.; Gu, C.; Zhang, W.; Sun, Y.; Sun, J.; Zhu, W.; Guo, X. Multistep nucleation and growth mechanisms of organic crystals from amorphous solid states. *Nat. Commun.* **2019**, *10*, 3872.
(106) El Abbassi, M.; Sangtarash, S.; Liu, X.; Perrin, M. L.; Braun, O.; Lambert, C.; van der Zant, H. S. J.; Yitzchaik, S.; Decurtins, S.; Liu, S.-X.; Sadeghi, H.; Calame, M. Robust graphene-based molecular devices. *Nat. Nanotechnol.* **2019**, *14*, 957−961.
(107) Zhang, Y.-P.; Chen, L.-C.; Zhang, Z.-Q.; Cao, J.-J.; Tang, C.; Liu, J.; Duan, L.-L.; Huo, Y.; Shao, X.; Hong, W.; Zhang, H.-L. Distinguishing diketopyrrolopyrrole isomers in single-molecule junctions via reversible stimuli-responsive quantum interference. *J. Am. Chem. Soc.* **2018**, *140*, 6531−6535.
(108) Wang, Y.; Frasconi, M.; Liu, W.-G.; Sun, J.; Wu, Y.; Nassar, M. S.; Botros, Y. Y.; Goddard, W. A., III; Wasielewski, M. R.; Stoddart, J. F. Oligorotaxane radicals under orders. *ACS Cent. Sci.* **2016**, *2*, 89−98.
(109) Li, S.; Li, J.; Yu, H.; Pudar, S.; Li, B.; Rodríguez-López, J.; Moore, J. S.; Schroeder, C. M. Characterizing intermolecular interactions in redox-active pyridinium-based molecular junctions. *J. Electroanal. Chem.* **2020**, *875*, 114070.
(110) Yu, H.; Luo, Y.; Beverly, K.; Stoddart, J. F.; Tseng, H. R.; Heath, J. R. The molecule−electrode interface in single-molecule transistors. *Angew. Chem., Int. Ed.* **2003**, *42*, 5706−5711.
(111) Scott, G. D.; Chichak, K. S.; Peters, A. J.; Cantrill, S. J.; Stoddart, J. F.; Jiang, H. Mechanism of enhanced rectification in unimolecular Borromean ring devices. *Phys. Rev. B* **2006**, *74*, 113404.
(112) Xin, N.; Guan, J.; Zhou, C.; Chen, X.; Gu, C.; Li, Y.; Ratner, M. A.; Nitzan, A.; Stoddart, J. F.; Guo, X. Concepts in the design and engineering of single-molecule electronic devices. *Nat. Rev. Phys.* **2019**, *1*, 211−230.
(113) Xiang, D.; Wang, X.; Jia, C.; Lee, T.; Guo, X. Molecular-scale electronics: from concept to function. *Chem. Rev.* **2016**, *116*, 4318−4440.
(114) Ye, T.; Kumar, A. S.; Saha, S.; Takami, T.; Huang, T. J.; Stoddart, J. F.; Weiss, P. S. Changing stations in single bistable rotaxane molecules under electrochemical control. *ACS Nano* **2010**, *4*, 3697−3701.
(115) Li, Y.; Yang, C.; Guo, X. Single-molecule electrical detection: a promising route toward the fundamental limits of chemistry and life science. *Acc. Chem. Res.* **2020**, *53*, 159−169.

https://doi.org/10.1021/acsanm.2c01880
ACS Appl. Nano Mater. 2022, 5, 13874−13886